Structures of Class A Macrophage Scavenger Receptors

ELECTRON MICROSCOPIC STUDY OF FLEXIBLE, MULTIDOMAIN, FIBROUS PROTEINS AND DETERMINATION OF THE DISULFIDE BOND PATTERN OF THE SCAVENGER RECEPTOR CYSTEINE-RICH DOMAIN*

David Resnick‡§, Jon E. Chatterton‡, Karen Schwartz¶‖, Henry Slayter, and Monty Krieger‡ ‡‡**

*From the ‡Department of Biology, Massachusetts Institute of Technology, Cambridge, Massachusetts 02139, ¶Arris Pharmaceutical Corporation, South San Francisco, California 94080, and the **Dana-Farber Cancer Institute, Boston, Massachusetts 02115*

Structures of secreted forms of the human type I and II class A macrophage scavenger receptors were studied using biochemical and biophysical methods. Proteolytic analysis was used to determine the intramolecular disulfide bonds in the type I-specific scavenger receptor cysteine-rich (SRCR) domain: $Cys^2–Cys^7$, $Cys^3–Cys^8$, and $Cys^5–Cys^6$. This pattern is likely to be shared by the highly homologous domains in the many other members of the SRCR domain superfamily. Electron microscopy using rotary shadowing and negative staining showed that the type I and II receptors are extended molecules whose contour lengths are ~440 Å. They comprised two adjacent fibrous segments, an α-helical coiled-coil (~230 Å, including a contribution from the N-terminal spacer domain) and a collagenous triple helix (~210 Å). The type I molecules also contained a C-terminal globular structure (~58 × 76 Å) composed of three SRCR domains. The fibrous domains were joined by an extremely flexible hinge. The angle between these domains varied from 0 to 180° and depended on the conditions of sample preparation. Unexpectedly, at physiologic pH, the prevalent angle seen using rotary shadowing was 0°, resulting in a structure that is significantly more compact than previously suggested. The apparent juxtaposition of the fibrous domains at neutral pH provides a framework for future structure-function studies of these unusual multiligand receptors.

The type I and II class A macrophage scavenger receptors (SR-AI and SR-AII)[1] are trimeric integral membrane glycoproteins that exhibit unusual ligand binding properties (Krieger and Herz, 1994). They bind a diverse array of macromolecules or macromolecular complexes, whose only common property is that they are polyanionic. These ligands include modified lipoproteins (acetylated or oxidized low density lipoprotein), bacterial surface lipids (endotoxin and lipoteichoic acid), certain polynucleotides (poly(G) and poly(I), but not poly(C)), and some sulfated polysaccharides (fucoidan and dextran sulfate, but not heparin or chondroitin sulfate). A number of studies have suggested that these receptors may play a role in a wide variety of macrophage-associated physiologic and pathophysiologic processes (Krieger and Herz, 1994).

SR-AI and SR-AII are the alternatively spliced products of a single gene (Freeman *et al.*, 1990; Emi *et al.*, 1993). Based on their amino acid sequences deduced from cDNA clones from four species (Kodama *et al.*, 1990; Rohrer *et al.*, 1990; Matsumoto *et al.*, 1990; Freeman *et al.*, 1990; Ashkenas *et al.*, 1993), SR-AI and SR-AII were predicted to contain six distinct structural domains (Kodama *et al.*, 1990; Rohrer *et al.*, 1990; Ashkenas *et al.*, 1993): I, an amino-terminal cytoplasmic domain; II, a single transmembrane domain; III, a spacer domain; IV, an α-helical coiled-coil domain; V, a collagenous domain; and VI, an isotype-specific C-terminal domain of variable length. Domains I–V are identical in SR-AI and SR-AII. In SR-AII, domain VI consists of a poorly conserved, short sequence (6–17 amino acids) with no remarkable features. In SR-AI, domain VI is 110 residues long and includes an 8-residue connector followed by a 102-residue region called the scavenger receptor cysteine-rich (SRCR) domain.

The SRCR domain in SR-AI helped to define the ancient, highly conserved SRCR domain superfamily (Freeman *et al.*, 1990), which currently includes 14 proteins containing 52 independent SRCR domains (Resnick *et al.*, 1994; Li and Snyder, 1995; Kitamoto *et al.*, 1994; Elomaa *et al.*, 1995; Nunes *et al.*, 1995; Cheng *et al.*, 1996).[2] The functions of the SRCR domains in these diverse proteins, including SR-AI, are for the most part undefined; however, it has been proposed that these domains may participate in ligand binding interactions, as has recently been shown for one of the SRCR domains in CD6 (Whitney *et al.*, 1995). Studies of the structural features of an SRCR domain from a single member of the superfamily should provide insights into the structures of similar domains in other superfamily members.

The detailed analysis of the structures of class A scavenger receptors has been limited by the inability to obtain adequate amounts of protein and by technical difficulties inherent in working with water-insoluble integral membrane molecules. To circumvent these problems, we have generated stable CHO

§ Howard Hughes Medical Institute Predoctoral Fellow.

‖ Present address: Stanford University School of Medicine, Palo Alto, CA 94305.

‡‡ To whom correspondence should be addressed: Dept. of Biology, Rm. 68-483, MIT, 77 Massachusetts Ave., Cambridge, MA 02139. Tel.: 617-253-6793; Fax: 617-258-5851.

[1] The abbreviations used are: SR-AI and SR-AII, type I and II class A macrophage scavenger receptors, respectively; s-hSR-AI and s-hSR-AII, secreted human SR-AI and SR-AII, respectively; SRCR, scavenger receptor cysteine-rich; CHO, Chinese hamster ovary; FBS, fetal bovine serum; HPLC, high pressure liquid chromatography.

[2] W. E. Mayer, and H. Tichy, (1995) GenBank™ accession number U20652.

cell lines that overexpress truncated secreted forms of the human class A scavenger receptors (s-hSR-AI and s-hSR-AII). We have used purified s-hSR-AI to initiate studies of the covalent structure of the SRCR domain. In addition, we have examined the structures of s-hSR-AI and s-hSR-AII using electron microscopy. Analysis of the single molecule images supports the proposed scavenger receptor domain structure described above and provides the first view of globular SRCR domains. Unexpectedly, the microscopy suggests that, at physiologic pH, there may be substantial lateral interactions between the α-helical coiled-coil and collagenous domains.

EXPERIMENTAL PROCEDURES

Materials

CHO[DHFR$^-$] cells were obtained from American Type Culture Collection. Lysyl endopeptidase from *Achromobacter lyticus* (Lys-C), modified trypsin, and sequencing-grade protease V8 (Glu-C) were obtained from Wako Bioproducts, Promega, and Boehringer Mannheim, respectively. Uranyl acetate was obtained from Polyscience. Mica sheets (1 × 4 cm), graphite rods (for carbon evaporation), 500-mesh copper grids, and a diffraction grating replica with latex spheres were purchased from Ted Pella, Inc. Poly(G) beads and other reagents were obtained as described previously (Resnick *et al.*, 1993).

Construction of pRc/CMV-s-hSR-AI and pRc/CMV-s-hSR-AII Expression Vectors

cDNAs encoding soluble forms of the human type I and II class A macrophage scavenger receptors were generated by polymerase chain reaction using a human SR-A cDNA (generously provided by Dr. T. Kodama) and a 5′-oligonucleotide encoding a sequence comprising the myelin-associated glycoprotein leader sequence (Arquint *et al.*, 1987) as well as a FLAG epitope tag (type II receptor only) (Hopp *et al.*, 1988) and overlapping the SR-A cDNAs by 21 bases starting at the lysine at base position 230 (Matsumoto *et al.*, 1990). The 3′-oligonucleotides contained the last 21 bases of the type I or II receptors followed by an *Xba*I restriction site. The blunt/*Xba*I fragment was ligated to pRc/CMV (Invitrogen) at the *Hind*III (blunt)/*Xba*I sites. The constructs were named pRc/CMV-s-hSR-AI and pRc/CMV-s-hSR-AII. After cleavage of the signal sequence, the N-terminal sequence of the type II expressed protein is predicted to be DYKDDDDKK^{77}-, where Lys^{77} is the first residue contributed by the scavenger receptor, while Lys^{77} is predicted to be at the amino terminus of the type I receptor.

Cell Culture, Transfections, and Dihydrofolate Reductase Amplification

All incubations with intact cells were performed at 37 °C in a humidified 5% CO_2 incubator. Stock cultures of CHO[DHFR$^-$] cells were grown in medium A (Iscove's modified Dulbecco's medium supplemented with 100 units/ml penicillin, 100 μg/ml streptomycin, 10^{-4} M hypoxanthine, 10^{-5} M thymidine, and 2 mM glutamine) containing 10% (v/v) fetal bovine serum (FBS) (medium B).

Transfectants expressing s-hSR-AI (CHO[s-hSR-AI]) were generated using the Lipofectin method as suggested by the manufacturer (Life Technologies, Inc.). On day 0, CHO[DHFR$^-$] cells were plated at 10^6 cells/100-mm dish in medium B. On day 1, the cells were washed twice with Dulbecco's complete phosphate-buffered saline (Life Technologies, Inc.) and refed with a transfection mixture containing 5 ml of medium A with 100 μl of Lipofectin, 10 μg of *Bgl*II-linearized pRc/CMV-s-hSR-I, and 200 ng of *Bam*HI-linearized pSV2-dhfr (Subramani *et al.*, 1981). Following a 5-h incubation, 5 ml of medium A containing 20% (v/v) FBS were added. On day 2, the cells were refed with medium B; and on day 3, cells were harvested with trypsin and plated at 2×10^5 to 1×10^6 cells/100-mm dish in medium C (Iscove's modified Dulbecco's medium supplemented with 100 units/ml penicillin, 100 μg/ml streptomycin, 2 mM glutamine, and 0.5 mg/ml Geneticin (Life Technologies, Inc.)) containing 7% (v/v) FBS, which was extensively dialyzed against 150 mM NaCl (medium D). On day 4, colonies were switched to medium C containing 10% dialyzed FBS and 50 nM methotrexate (Sigma). Cells expressing increasingly higher levels of s-hSR were selected by progressively increasing the concentration of methotrexate and rescreening for expression using metabolic labeling and a poly(G) solid-state bead binding assay as described previously (Resnick *et al.*, 1993). One positive clone, designated CHO[s-hSR-AI] (clone 38-2-19), was resistant to 1 μM methotrexate and expressed high levels of s-hSR-AI. It was used for all experiments involving s-hSR-AI.
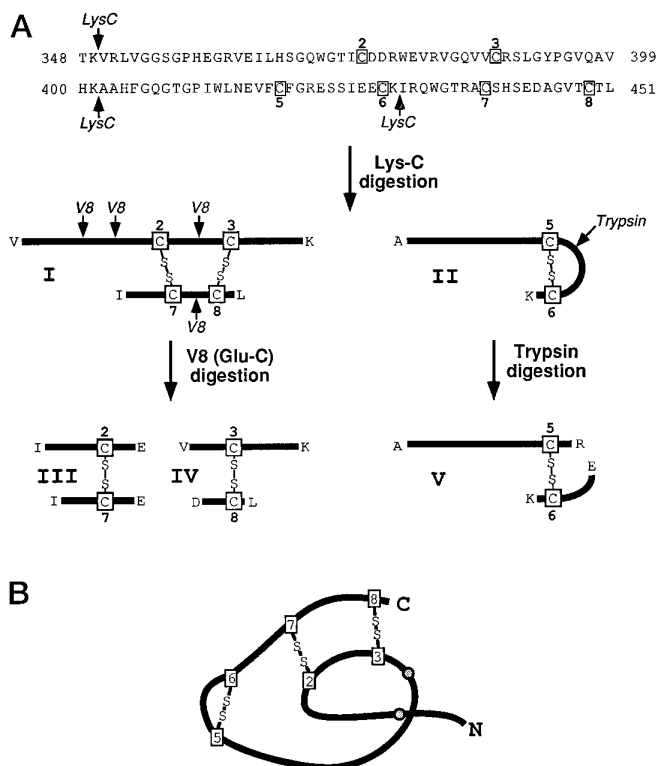
FIG. 1. **Identification of disulfide bonds in the SRCR domain.** Purified s-hSR-AI was subjected to proteolytic digestion with Lys-C as described under "Experimental Procedures." *A*, shown at the top are this enzyme's target sites in the SRCR sequence, with amino acids numbered as in the full-length protein. Following cleavage with Lys-C, fragments I and II were identified as reduction-sensitive peaks by reverse-phase HPLC and further characterized using both N-terminal sequencing and amino acid analysis. Peak I was digested with protease V8, and the resulting peptides were resolved by HPLC, yielding fragments III and IV. Peak II was digested with trypsin, yielding peak V. The identities of peaks III–V were determined using mass spectrometry and either amino acid analysis or N-terminal sequencing. Peak identification data are as follows. Peak I: observed N-terminal sequence, (I/V)R(L/Q)VG, and predicted, (I/V)R(L/Q)(V/W)G; amino acid analysis average deviation from predicted value = 11%. Peak II: observed N-terminal sequence, A(AX)HFG, and predicted, AAHFG; amino acid analysis average deviation = 23%; observed M_r = 3211 and predicted M_r = 3212. Peak III: observed M_r = 3440 and predicted M_r = 3445; amino acid analysis average deviation = 13.5%. Peak IV: observed N-terminal sequence, (D/V)(A/R)(G/V)(G/V)(Q/T), and predicted, (D/V)(A/R)(G/V)(G/V)(Q/T); observed M_r = 3033 and predicted M_r = 3030. Peak V: observed M_r = 3233 (also 3273) and predicted M_r = 3230; amino acid analysis average deviation = 10.2%. *B*, shown is a model of the disulfide interactions obtained using the approach shown in *A*. *Stippled circles* indicate the locations corresponding to those of cysteines 1 and 4, which are not present in the SRCR domain of SR-AI, but are found in SRCR domains from several other proteins (Resnick *et al.*, 1994).

Transfectants expressing s-hSR-AII (CHO[s-hSR-AII]) were generated using a variation of the Lipofectin method. CHO[DHFR$^-$] cells were grown in Ham's F-12 medium instead of Iscove's modified Dulbecco's medium. Cells were plated at a density of 5×10^6 cells/100-mm dish prior to transfection. Colonies were screened by Western blotting using an antipeptide antibody raised against a C-terminal peptide of hSR-AII. A high expression cell line, CHO[s-hSR-AII]clone 201-16, resistant to 5 μM methotrexate, was obtained by amplifying with increasing concentrations of methotrexate and was used to generate s-hSR-AII.

Expression and Purification of s-hSR-AI and s-hSR-AII

Expression—Cells were set in 850-cm^2 roller bottles in medium E (Ham's F-12 medium containing 10% FBS, 100 units/ml penicillin, 100 μg/ml streptomycin, and 2 mM glutamine) at a density of 10^7 cells/bottle. Cells were grown to ~50% confluence and were then washed twice with complete phosphate-buffered saline and refed with 200 ml of medium F (50% Ham's F-12 medium, 50% Dulbecco's modified Eagle's medium, 100 units/ml penicillin, 100 μg/ml streptomycin, 2 mM gluta-
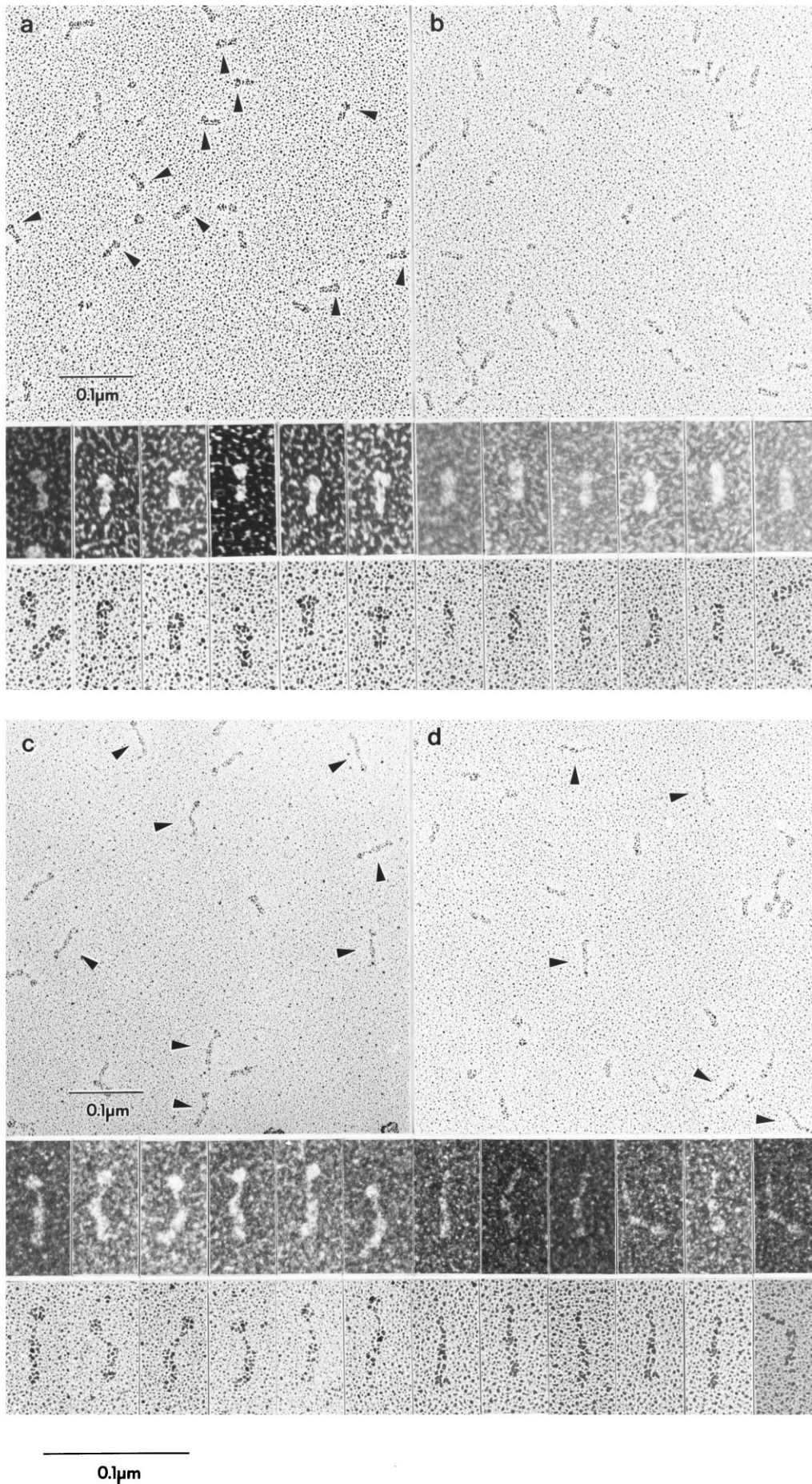
FIG. 2

mine, 10 mM HEPES, pH 7.4, and 1 mM sodium butyrate). Four days later, the cells were refed and incubated for an additional 4 days. The culture media were then collected and, after addition of sodium azide (final concentration of 0.01% (w/v)), were clarified by centrifugation (4000 × *g* for 15 min at 4 °C) and stored at 4 or −20 °C.

Purification—All steps were carried out at 4 °C. Culture media were concentrated using a spiral cartridge ultrafiltration apparatus (Amicon, Inc.) fitted with an S1Y100 membrane (approximate molecular mass cutoff of 100 kDa). Following concentration of 4–14 liters to ~350 ml, the concentrate was diafiltered against 6 liters of 50 mM ammonium bicarbonate, pH 7.5, and further concentrated to a final volume of 125 ml, all in the same device. The sample was then clarified by centrifugation (4000 × *g* for 30 min). The supernatant was passed through a 0.45 μm filter and then was applied at a flow rate of 0.75 ml/min to a 6 × 1.5-cm column containing 10 ml of poly(G) resin (Sigma) that had been equilibrated in 5% Buffer A (1 M ammonium bicarbonate, pH 7.5) and 95% H₂O. The column was washed with 50 ml of 5% Buffer A and eluted at 0.5 ml/min with a 95-ml linear gradient containing 5–100% Buffer A. The effluent was monitored at 280 nm, and those fractions containing protein were analyzed by 10% SDS-polyacrylamide gel electrophoresis and silver staining (Kozarsky *et al.*, 1986; Morrissey, 1981). Fractions containing s-hSR-A were pooled, diluted 1:1 with H₂O, and applied at 1 ml/min to a Mono Q HR5/5 column (Pharmacia Biotech Inc.) that had been pre-equilibrated in 7.5% Buffer A and 92.5% H₂O. The column was then washed with 30 ml of 7.5% Buffer A at 2 ml/min and eluted at 1 ml/min with a 40-ml 7.5–100% linear gradient of Buffer A in H₂O. The eluant was monitored at 280 nm and analyzed by gel electrophoresis as described above; fractions containing s-hSR-A were pooled. Yields were ~10.6 mg from 14 liters of s-hSR-AI medium and 10.8 mg from 4 liters of s-hSR-AII medium.

Disulfide Mapping of the SRCR Domain of s-hSR-AI

Urea (final concentration of 6 M) was added to 200 μg of s-hSR-AI, and the sample was submerged in boiling water for 20 min and then cooled to room temperature.

Lys-C Digestion—The urea concentration was lowered to 4 M by addition of Tris, pH 9.0 (final concentration of 0.1 M), and then Lys-C was added at an enzyme/s-hSR-AI ratio of ~1:45 (w/w). Following incubation at 37 °C for 4–13 h, peptides were resolved using HPLC (Hewlett-Packard 1090 system). In some cases, the samples were reduced by boiling in the presence of 100 mM dithiothreitol for 20 min prior to chromatography. Samples were applied at 1 ml/min to an analytical C₁₈ column (Vydac 218TP54), which was then washed for 5 min with H₂O, 0.1% trifluoroacetic acid and eluted with a linear gradient containing 0–60% acetonitrile and 0.1% trifluoroacetic acid. Peaks containing disulfides were identified by mobility changes upon reduction and by comparison with digests of the type II receptor, which lacks the SRCR domain. The composition of these peaks was determined by both N-terminal sequencing and analysis of the amino acid composition (performed by the Biopolymers Laboratory, Department of Biology, Massachusetts Institute of Technology). Fractions containing these peptides were isolated and further characterized. Prior to additional proteolytic digestion, the fractions were evaporated to dryness (Speed-Vac) and dissolved in 8 M urea by boiling for 20 min.

Protease V8 (Glu-C) Digestions—HPLC-purified fragments of s-hSR-AI were diluted in 25 mM NH₄HCO₃, pH 7.5, to reduce the urea concentration to 1 M and digested with 1 μg of enzyme for 10 h at 37 °C. Peptides were resolved by reverse-phase HPLC as described above and analyzed by mass spectrometry using matrix-assisted laser desorption with a time of flight detector analysis (Howard Hughes Medical Institute Biopolymers Facility, Harvard Medical School) and either amino acid analysis or N-terminal sequencing.

Trypsin Digestions—HPLC-purified fragments of s-hSR-AI were diluted in 50 mM Tris and 1 mM CaCl₂, pH 7.6, to reduce the urea concentration to 1 M and digested with 1 μg of enzyme for 10 h at 37 °C. Products were analyzed as described above.

Electron Microscopy

Negatively stained specimens were prepared using the pleated sheet technique (Schumaker *et al.*, 1981; Smith and Seegan, 1984). Samples of s-hSR-AI and s-hSR-AII were diluted to 1 μg/ml in phosphate-buffered saline, pH 7.4, and adsorbed to a thin carbon film using the procedure of Valentine *et al.* (1968). The carbon film was then washed in deionized water for 5 s and pleated to ~25% of its original length in the presence of aqueous 1% (w/v) uranyl acetate, pH 4.3. The pleated carbon was transferred to a 500-mesh copper grid as described (Smith and Seegan, 1984); excess stain was removed using premoistened Whatman No. 1 filter paper; and the carbon-coated grid was allowed to dry for >1 h. Negatively stained specimens were observed in a JEOL JEM 1200EX II transmission electron microscope operating at 80 kV with a 100-μm second condenser aperture, a "spot size" of 2 μm, and a 100-μm objective aperture. Photographs were taken at magnifications ranging from ×40,000 to 60,000. Microscope magnification was calibrated using a diffraction grating replica (2160 lines/mm) and latex spheres (0.261 μm).

Rotary metal-shadowed specimens were prepared by mixing ~20 μg/ml solutions of s-hSR-AI or s-hSR-AII in 150 mM ammonium acetate (adjusted to pH 7.4 or 4.3 with acetic acid) with 0.25 volume of redistilled glycerol, spraying onto freshly cleaved mica, and drying *in vacuo* for 20 h. The dried mica sheets were then rotary-shadowed with platinum or tungsten by means of resistive or electron bombardment heating, respectively (Slayter, 1976, 1983). The estimated average metal-film mass thickness was 100 ng/cm² for tungsten and somewhat more for platinum. Samples were examined in a JEOL JEM 100CX electron microscope using a top entry stage with a 40-μm objective aperture at an accelerating voltage of 100 kV (dark field) or 80 kV (bright field). Micrographs were recorded at a magnification of ×40,000 (calibrated with a diffraction grating replica) and enlarged photographically to ×140,000. High resolution dark-field images were also obtained, from the lightly shadowed specimens, by using matched annular condenser and objective apertures (Slayter, 1989, 1991).

Measurements of individual negatively stained molecules were made by projecting the electron microscope negatives onto a Sigma-Scan digitizing board (Jandel Scientific; magnification × 22). Measurements of rotary metal-shadowed molecules were made directly from photographic enlargements using a micrometer eyepiece. All measurements obtained from rotary metal-shadowed specimens were corrected for metal thickness. The measurements for the rotary metal-shadowed and negatively stained molecules were made independently by different individuals.

RESULTS AND DISCUSSION

Expression and Purification of Secreted Scavenger Receptors—To prepare substantial amounts of the extracellular domains of class A scavenger receptors, we generated stable amplified CHO[DHFR⁻] cell lines expressing high levels of secreted forms of the human type I (CHO[s-hSR-AI]) and type II (CHO[s-hSR-AII]) receptors (see "Experimental Procedures"). To facilitate secretion of the soluble extracellular domains, we constructed a cDNA expression vector in which the sequences encoding the cytoplasmic and transmembrane domains were replaced with one encoding a myelin-associated glycoprotein signal sequence, linked to the SR-A protein either directly (s-hSR-AI) or by a FLAG epitope tag (s-hSR-AII). Removal of the signal sequence from the protein product in transfected cells was confirmed by amino-terminal sequencing in the case of the type I receptor. The calculated molecular mass of the type I secreted receptor (s-hSR-AI) is 42.3 kDa (375 amino acids), while that of the type II secreted receptor (s-hSR-AII) is 32.1 kDa (290 amino acids). The secreted proteins were purified by chromatographic methods (see "Experimental Proce-

FIG. 2. **Rotary-shadowed images of s-hSR-AI and s-hSR-AII.** Samples of purified s-hSR-AI or s-hSR-AII were prepared for rotary metal shadowing as described under "Experimental Procedures" at pH 7.4 or 4.3 and visualized using transmission electron microscopy. In each panel, the *top* and *bottom rows* were shadowed with platinum and visualized using bright-field optics; the *middle row* was shadowed with minimal tungsten and visualized using dark-field optics. *a*, s-hSR-AI at pH 7.4. *Arrowheads* indicate the globular structures observed at the ends of the type I molecules. *b*, s-hSR-AII at pH 7.4. *c*, s-hSR-AI at pH 4.3. *Arrowheads* indicate the junction between the thick and thin fibrous segments. *d*, s-hSR-AII at pH 4.3. *Arrowheads* indicate the junction between the thick and thin fibrous segments. *Shorter scale bars* are for the *top row* of each panel; *longer scale bars* are for the *middle* and *bottom rows* of each panel.
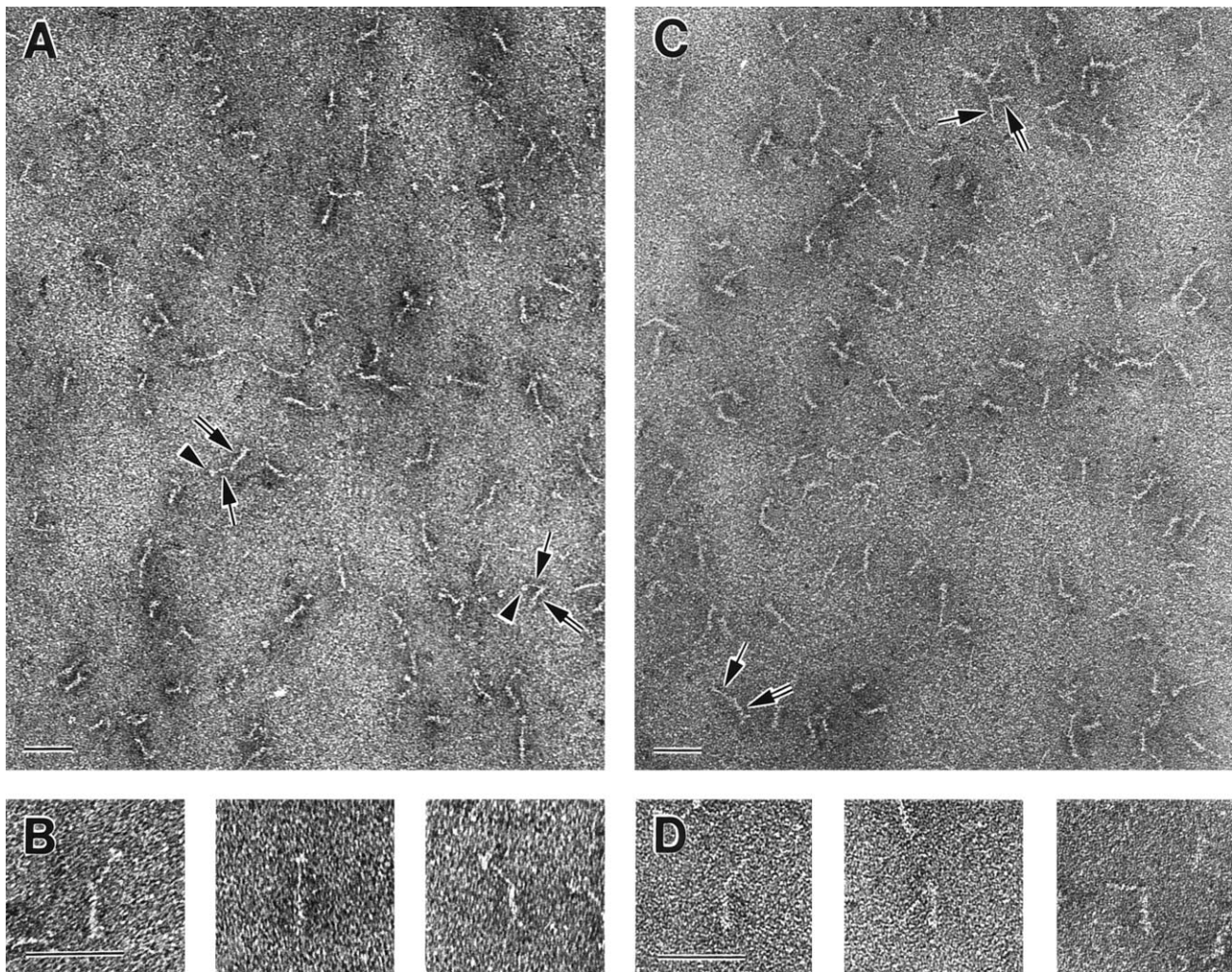
FIG. 3. **Negatively stained images of s-hSR-AI and s-hSR-AII.** Samples of purified s-hSR-AI or s-hSR-AII were prepared as described under "Experimental Procedures" and visualized using transmission electron microscopy. *Double-tailed arrows* indicate coiled-coil/spacer domains (thick fibrous segments); *single-tailed arrows* indicate collagenous domains (thin fibrous segments); and *arrowheads* indicate SRCR domains (s-hSR-AI only). *A* and *B*, s-hSR-AI; *C* and *D*, s-hSR-AII. *Bars* indicate 0.05 μm.

dures") to >95% homogeneity, as evaluated either by HPLC or by SDS-polyacrylamide gel electrophoresis and silver staining (data not shown). Yields were ~0.75 mg of purified s-hSR-AI/liter of culture medium and 2.7 mg of s-hSR-AII/liter. The secreted receptors were examined using a solid-state binding assay (Resnick *et al.*, 1993) and exhibited ligand binding activity with the expected polyanion specificity (data not shown).

Disulfide Linkages in the SRCR Domain—The pattern of disulfide bonds in the SRCR domain of s-hSR-AI was determined by sequentially cleaving the protein with proteases (Lys-C followed by protease V8 or trypsin) and determining the composition of the relevant peptide products using amino acid analysis, mass spectrometry, and/or N-terminal sequencing as described under "Experimental Procedures." Digestion products were separated by HPLC, and the fractions containing disulfide-bond linked peptides were identified both by their reduction sensitivity and by comparison with digests from s-hSR-AII (which lacks the SRCR domain). The experimental strategy and the results are summarized in Fig. 1. The six cysteines in the SRCR domain of SR-AI are numbered 2, 3, 5, 6, 7, and 8, as described by Resnick *et al.* (1994). SRCR domains fall into two groups: those (such as that in SR-AI) without cysteines 1 and 4 and those with them (Resnick *et al.*, 1994). Two reduction-sensitive products of the Lys-C digestion, designated peptides I and II (Fig. 1), were identified by amino acid

analysis and N-terminal sequencing. Unambiguous assignment of disulfide bonds required further proteolytic digestion. Peptide I was digested with protease V8 and subjected to reverse-phase HPLC, and disulfide-containing peaks were again identified. Analysis of these peaks using either mass spectrometry and amino acid analysis (peptide III) or mass spectrometry and N-terminal sequencing (peptide IV) allowed unambiguous assignment of the disulfide bridges as Cys^2–Cys^7 and Cys^3–Cys^8. Digestion of peptide II with trypsin followed by reverse-phase HPLC yielded peptide V, and both amino acid analysis and mass spectrometry established the presence of the Cys^5–Cys^6 disulfide bond. A model for the disulfide bond pattern is shown in Fig. 1*B*.

This disulfide bond pattern is consistent with the prediction of a Cys^2–Cys^7 disulfide bond made based on sequence comparisons of many different SRCR family members (Resnick *et al.*, 1994). It seems highly likely that all 52 SRCR domains identified to date share the disulfide bond pattern established here for the SRCR domain of SR-AI and that cysteines 1 and 4 (shown as *stippled circles* in Fig. 1*B*) form a disulfide in those SRCR domains that have all eight cysteines. Determination of the disulfide bond arrangement in the scavenger receptor SRCR domain will facilitate future analysis of SRCR domain structure. In the absence of a functional assay, the disulfide bond arrangement can be used as an indicator of correct folding

of recombinant SRCR domains. Experiments are in progress to generate large quantities of SRCR domains for higher resolution structural analysis of this increasingly widespread structural motif.

Electron Microscopy of s-hSR-AI and s-hSR-AII—Rotary metal-shadowed specimens of the type I and II secreted receptors were examined by transmission electron microscopy (Fig. 2, *a* and *b*). In specimens prepared at pH 7.4, the type II receptor (Fig. 2*b*) formed a relatively featureless rod, with dimensions of 260 ± 29 Å $\times \sim 52$ Å. The type I receptor (Fig. 2*a*) was similar, except for the presence of a globular region at one end, giving the receptor a "lollipop" appearance. This globular feature presumably corresponds to three SRCR domains superposed on the rod segment. The overall length and width of the type I receptor were 250 ± 28 and 45 ± 15 Å, respectively, and the diameter of the globular domain was 68 ± 20 Å. Surprisingly, neither secreted scavenger receptor isoform resembled the structures of other proteins containing short collagenous sequences (Lu *et al.*, 1993). When examined at pH 7.4, both the type I and II receptors were shorter and wider than would be estimated from the primary structures of these receptors (Kodama *et al.*, 1990; Rohrer *et al.*, 1990) and crystal structures of related molecules (Harbury *et al.*, 1994; Bella *et al.*, 1994). Based on the predicted dimensions of the coiled-coil (181×24 Å) and collagenous domains (197×10 Å) (Harbury *et al.*, 1994; Bella *et al.*, 1994), the receptor would be expected to have an overall length of ~ 380 Å with a width ranging from 10 to 24 Å over much of its length.

Specimens of the type I and II secreted receptors were also examined in the electron microscope following negative staining with uranyl acetate, pH 4.3 (Fig. 3). In contrast to the results obtained by rotary metal shadowing (Fig. 2, *a* and *b*), the majority (77%) of the negatively stained molecules appeared to be composed of two fibrous segments that differed substantially in thickness, and the overall lengths were ~ 440 Å. Once again, the principal difference between the two isoforms was the presence in s-hSR-AI, but never in s-hSR-AII, of a globular domain at one end. This globular domain, which sometimes appeared to be resolved into two or, less frequently, three small subdomains (average subdomain dimensions of 54 ± 10 Å $\times 35 \pm 9$ Å, $n = 23$), was observed at the end of the thin segment, but never at the end of the thick segment. This globular domain almost certainly represents three SRCR domains. Therefore, we propose that the thin segment is the collagenous domain and the thick segment is the α-helical coiled-coil domain with a possible contribution from the spacer domain. We also observed a number of compact molecules in every negatively stained sample, whose average dimensions were similar to those of the thick fibrous segments and which may be related to the structures observed by rotary metal shadowing described above. In those negatively stained images in which both fibrous segments were resolved, the angle between the two segments ("hinge angle") ranged from 20 to 180°, with 80% of the molecules having angles >100°. Thus, there appears to be a flexible hinge linking the α-helical coiled-coil and collagenous domains, and there was some preference for molecules with a more extended conformation.

Length and width measurements were performed on the individual s-hSR-AI/II domains observed in negatively stained specimens (Fig. 4*A*). The average length of the thin segment in s-hSR-AII was similar to the predicted length of the collagenous domain; however, in s-hSR-AI, it was shorter, raising the possibility that the SRCR domains may partially obscure the C terminus of the collagenous domain in these images. The average lengths of the thick segments were somewhat longer than the predicted length of the α-helical coiled-coil domain,
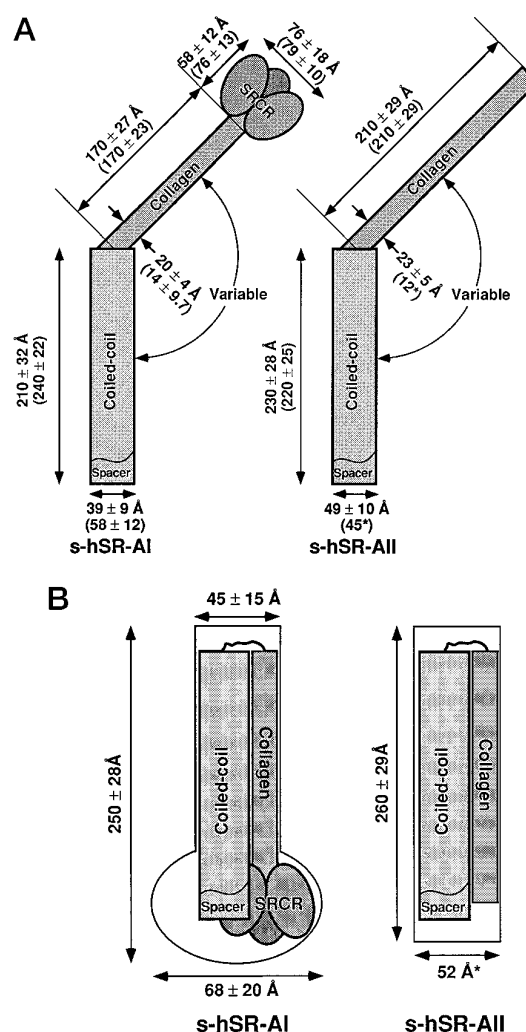
FIG. 4. **Models of s-hSR-AI and s-hSR-AII with dimensions based on negatively stained and rotary metal-shadowed samples visualized by electron microscopy.** *A*, extended forms. Dimensions (mean ± S.D.) are based on the measurements of >100 negatively stained images. The angle between the two fibrous domains (hinge angle) ranged from 20 to 180°, with 80% of the values >100°. Similar dimensions were obtained from measurements of >100 extended molecules observed using metal shadowing following exposure to low pH (indicated in *parentheses*). Widths of the metal-shadowed molecules were difficult to measure and, if marked by an *asterisk*, represent a best estimate where metal correction is relatively great. *B*, compact forms. Dimensions (mean ± S.D.) are based on the measurements of >58 metal-shadowed images.

possibly reflecting a contribution of the spacer domain. The measured widths (Fig. 4*A*) were almost 2-fold greater than the predicted widths. Absolute width measurements, however, are affected significantly by small errors, and the ratio of the measured widths of the two domains (2:1) is similar to the predicted ratio (2.4:1). Thus, the dimensions of the extended form of the receptor seen in negatively stained images provide strong support for the proposed domain structure of the receptor. Biochemical and biophysical data also support the proposed domain structure. Circular dichroism studies of s-hSR-AI and s-hSR-AII indicated that the receptors' α-helical content is consistent with the presence of the proposed α-helical coiled-coil domain (Resnick, 1996). Amino acid analysis revealed the presence of significant amounts of hydroxylated lysine and proline, consistent with the presence of a collagenous structure (Resnick, 1996).

It appears likely that the more compact structures for s-hSR-AI and s-hSR-AII visualized by rotary metal shadowing,

Structure of Class A Scavenger Receptors

relative to those seen using negative staining, are a consequence of the majority of the molecules bending back on themselves with a hinge angle of 0°. Differences in pH during sample preparation might account for the differences in the preferred hinge angles observed using rotary metal shadowing and negative staining. During negative stain specimen preparation, the molecules were deposited on the carbon support film in a pH 7.4 buffer and then exposed briefly to aqueous uranyl acetate at pH 4.3. The molecules viewed after metal shadowing were not exposed to the low pH. However, to determine if brief exposure to low pH might partially dissociate otherwise closely associated fibrous domains of these receptors, we dialyzed the secreted receptors against pH 4.3 buffer and examined their structures by rotary metal shadowing (Fig. 2, *c* and *d*). Low pH treatment transformed some, but not all, of the molecules into the more extended conformation seen by negative staining (Table I). The measurements of the dimensions of the fibrous segments in these images agreed closely with those obtained from the negatively stained molecules (Fig. 4*A*). Thus, the hinge separating the two fibrous domains must be extremely flexible, and the hinge angle has a range of 0–180°. At neutral pH, the preferred hinge angle is 0° in the metal-shadowed images. Brief exposure to low pH may disrupt favorable charge-charge interactions between the two fibrous domains and generate a more extended conformation in which the preferred hinge angle is >100°.

The functional relevance of the observed pH-dependent conformations of these molecules is not yet defined. Previous studies have shown that treatment by moderately low pH (~5–6.5) releases ligands from class A scavenger receptors (Naito *et al.*, 1991; Resnick *et al.*, 1993). If the conformational change observed here after exposure to pH 4.3 also occurs at pH 5–6.5, it might play a role in pH-dependent ligand release. Additional studies that extend this work to more physiologic pH values and an examination of the pH dependence of ligand binding to other collagenous structures (*e.g.* C1q and MARCO) will be required to explore this issue thoroughly. Further studies will also be required to determine if the compact structure observed here in truncated secreted forms of SR-A is present in the full-length molecules when they are embedded in the plasma membrane.

This study has provided the first insights into the structure of the class A scavenger receptor SRCR domain and, by extension, into the structures of the many other SRCR domains in a rapidly expanding superfamily of proteins. Studies of the secreted receptors by electron microscopic imaging of individual molecules have improved our understanding of their overall structure by confirming the domain model initially suggested by primary sequence analysis and by revealing that they can assume an unexpected, compact conformation at neutral pH. Further analysis of the functional significance of the compact form and potential pH-dependent conformational changes, as well as higher resolution structural studies, should provide additional insights into the structures and unusual binding properties of these multiligand/multifunction receptors.

REFERENCES

Arquint, M., Roder, J., Chia, L.-S., Down, J., Wilkinson, D., Bayley, H., Braun, P., and Dunn, R. (1987) *Proc. Natl. Acad. Sci. U. S. A.* **84,** 600–604
Ashkenas, J., Penman, M., Vasile, E., Freeman, M., and Krieger, M. (1993) *J. Lipid Res.* **34,** 983-1000
Bella, J., Eaton, M., Brodsky, B., and Berman, H. M. (1994) *Science* **264,** 75–81
Bickel, P. E., and Freeman, M. W. (1992) *J. Clin. Invest.* **90,** 1450–1457
Cheng, H., Bjerknes, M., and Chen, H. (1996) *Anat. Rec.* **244,** 327–343
Elomaa, O., Kangas, M., Sahlberg, C., Tuukkanen, J., Sormunen, R., Liakka, A., Thesleff, I., Kraal, G., and Tryggvason, K. (1995) *Cell* **80,** 603–609
Emi, M., Asaoka, H., Matsumoto, A., Hiroshige, I., Kurihara, Y., Wada, Y., Kanamori, H., Yazaki, Y., Takahashi, E., Lepert, M., Lalouel, J. M., Kodama, T., and Mukai, T. (1993) *J. Biol. Chem.* **268,** 2120–2125
Freeman, M., Ashkenas, J., Rees, D. J., Kingsley, D. M., Copeland, N. G., Jenkins, N. A., and Krieger, M. (1990) *Proc. Natl. Acad. Sci. U. S. A.* **87,** 8810–8814
Harbury, P. B., Kim, P. S., and Alber, T. (1994) *Nature* **371,** 80–83
Hopp, T. P., Prickett, K. S., Price, V., Libby, R. T., March, C. J., Cerretti, P., Urdal, D. L., and Conlon, P. J. (1988) *Bio/Technology* **6,** 1205–1210
Kitamoto, Y., Yuan, X., Wu, Q., McCourt, D. W., and Sadler, J. E. (1994) *Proc. Natl. Acad. Sci. U. S. A.* **91,** 7588–7592
Kodama, T., Freeman, M., Rohrer, L., Zabrecky, J., Matsudaira, P., and Krieger, M. (1990) *Nature* **343,** 531–535
Kozarsky, K., Brush, H., and Krieger, M. (1986) *J. Cell Biol.* **102,** 1567–1575
Krieger, M., and Herz, J. (1994) *Annu. Rev. Biochem.* **63,** 601–637
Li, X.-J., and Snyder, S. H. (1995) *J. Biol. Chem.* **270,** 17675–17679
Lu, J., Wiedemann, H., Timpl, R., and Reid, K. B. M. (1993) *Behring Inst. Mitt.* **93,** 6–16
Matsumoto, A., Naito, M., Itakura, H., Ikemoto, S., Asaoka, H., Hayakawa, I., Kanamori, H., Aburatani, H., Takaku, F., Suzuki, H., Kobari, Y., Miyai, T., Takahashi, K., Cohen, E. H., Wydro, R., Housman, D. E., and Kodama, T. (1990) *Proc. Natl. Acad. Sci. U. S. A.* **87,** 9133–9137
Morrissey, J. H. (1981) *Anal. Biochem.* **117,** 307–310
Naito, M., Kodama, T., Matsumoto, A., Doi, T., and Takahashi, K. (1991) *Am. J. Pathol.* **139,** 1411–1423
Nunes, D. P., Keates, A. C., Afdhal, N. H., and Offner, G. D. (1995) *Biochem. J.* **310,** 41–48
Resnick, D. (1996) *Structure and Function of Class A Macrophage Scavenger Receptors*. Ph.D. thesis, Massachusetts Institute of Technology
Resnick, D., Freedman, N. J., Xu, S., and Krieger, M. (1993) *J. Biol. Chem.* **268,** 3538–3545
Resnick, D., Pearson, A., and Krieger, M. (1994) *Trends Biochem. Sci.* **19,** 5–8
Rohrer, L., Freeman, M., Kodama, T., Penman, M., and Krieger, M. (1990) *Nature* **343,** 570–572
Schumaker, V. N., Poon, P. H., Seegan, G. W., and Smith, C. A. (1981) *J. Mol. Biol.* **148,** 191–197
Slayter, H. S. (1976) *Ultramicroscopy* **1,** 341–357
Slayter, H. S. (1983) *Ann. N. Y. Acad. Sci.* **408,** 131–145
Slayter, H. S. (1989) *Methods Enzymol.* **169,** 326–335
Slayter, H. S. (1991) in *Electron Microscopy of Tissues, Cells, and Organelles: A Practical Approach* (Harris, J. R., ed) pp. 151–172, Oxford University Press, Oxford
Smith, C. A., and Seegan, G. W. (1984) *J. Ultrastruct. Res.* **89,** 111–122
Subramani, S., Mulligan, R., and Berg, P. (1981) *Mol. Cell. Biol.* **1,** 854–864
Valentine, R. C., Shapiro, B. M., and Stadtman, E. R. (1968) *Biochemistry* **7,** 2143–2152
Whitney, G. S., Starling, G. C., Bowen, M. A., Modrell, B., Siadak, A. W., and Aruffo, A. (1995) *J. Biol. Chem.* **270,** 18187–18190